# Design and fabrication of Fresnel zone plates with large numbers of zones

Z. Chen, Y. Vladimirsky, M. Brown, Q. Leonard, O. Vladimirsky, F. Moore, and F. Cerrina
*Center For X-ray Lithography, 3731 Schneider Drive, Stoughton, Wisconsin 53589-3097*

B. Lai, W. Yun, and E. Gluskin
*Advanced Photon Source, Argonne National Laboratory, Argonne, Illinois 60439*

(Received 12 August 1997; accepted 12 August 1997)

The advent of high-brightness x-ray sources in the 10–40 keV region opens new possibilities of experiments with microbeams. Techniques to form these focused beams may be based on glancing mirrors, phase elements, or diffractive optics, in particular Fresnel zone plates (FZPs). Because of the long focal length and large acceptance, FZPs designed to work in the hard x-ray region tend to have quite large diameters and large numbers of zones. For instance, the zone plate described in this article has a 1860 $\mu$m diam, a focal length of $f=3$ m (for 8 keV), and 1860 zones. On a standard pattern generator, circular shapes are always approximated as simpler structures. The tolerance requirement for shape and positions of zones depends on the number of zones, and it is necessary to guarantee that the circular structures are approximated to the required degree of accuracy while keeping the size of the data structure to a reasonable size for processing by the exposure system. For instance, if polygons are used to approximate circular zones, a formula for the minimum acceptable number of polygon sides can be derived. An x-ray mask for a Fresnel phase zone plate (FPZP) with 1860 zones was designed directly in Cambridge source pattern data format and fabricated using the Leica Cambridge e-beam tool installed in the CXrL. The zone plates presented in this article were designed for hard x rays, and multilevel x-ray lithography was employed as a fabrication technique to form absorber thickness sufficient to provide the necessary phase shift. Minimum gold features of 0.25 $\mu$m with thicknesses of 1.6 and 3 $\mu$m, were formed to be used with 8 and 20 keV photons, respectively. Finally, in order to estimate the quality of the zone plates during fabrication, a scanning electron microscope based moiré method was used.  [S0734-211X(97)12706-8]

## I. INTRODUCTION

Fresnel zone plates (FZPs) are widely used as focusing elements in soft x-ray microscopy,[1–3] and the fabrication techniques for a FZP working in the soft x-ray region are well established.[1,3–7] The interest in hard x-ray microscopy was boosted by the development of third generation synchrotron sources and by progress in the fabrication of thick high-resolution structures.[8–10] These phase and blazed zone plates with high efficiency and submicron resolution are being used in hard x-ray microfocusing applications, such as microanalysis, microdiffraction, microspectroscopy, and microimaging.[11]

The availability of high-brightness focused beams can substantially reduce exposure and image acquisition time. In general, there are two ways to increase the intensity of a focused beam: improving the diffraction efficiency or increasing the collecting area of a zone plate. In order to achieve high efficiency, FZPs for hard x rays must have an absorber thickness able to provide a $\sim\pi$ optical phase shift.[12] For the energy region from 8 to 20 keV, this translates into a range of gold absorber thicknesses from 1.6 to 3.5 $\mu$m. Using nickel as a phase shifting material would require a thickness from 3.5 to 7.0 $\mu$m for the same energy region.[8] At the same time, to provide high spatial resolution, the outermost zone width of a Fresnel phase zone plate (FPZP) has to be in the submicron region, requiring advanced lithographic techniques. X-ray lithography, which is capable of providing sub-100 nm resolution and high aspect ratio patterns due to low x-ray absorption in photoresist,[8,9] is a natural candidate for the fabrication of these structures. Indeed, blazed zone plates with focusing efficiency up to 80% have been fabricated using aligned multilevel x-ray exposures at CXrL.[10]

In order to increase the x-ray flux $I$ one needs to increase the illuminated area $A$:

$$I \propto A = \pi r_N^2 \simeq \pi N \lambda f. \tag{1}$$

Hence, an intensity increase in the focus requires a larger number of zones $N$, and (for a given resolution) longer focal distance $f$. In the case when $\lambda=0.155$ nm, $f=3$ m, and $\delta r=0.25$ $\mu$m, the number of zones is 1860. Fabrication of x-ray zone plates is based mostly on e-beam writing. In this step, the circular shapes are approximated by polygonal areas, thus, prompting the question of the influence of the approximation on the quality of the image and on the focusing efficiency.

In the following sections, we present our approach to e-beam layout and writing of a large zone plate pattern, FPZP replication using x-ray lithographic techniques, and the evaluation of zone plates.[13] We show that the zone shape approximation is critical for a large number of zones, and the tolerance requirements will be also addressed and discussed in this article.

## II. E-BEAM WRITING

### A. FPZP design and data preparation

The zone plate described in this article has a diameter of 1860 $\mu$m, an outermost zone width $\delta r_N = 0.25$ $\mu$m, a focal length $f = 3$ m (for 8 keV), and 1860 zones. When the product $N\lambda$ is small compared to $f$, the second term in the zone plate equation

$$r_N^2 = N\lambda f + N^2\lambda^2/4 \tag{2}$$

can be neglected. However, as will be shown, the dimensional tolerance of the zone shape and placement depends on the number of zones.

When circular patterns are mapped onto the orthogonal Cartesian coordinates used by an e-beam positioning system, several issues must be taken into consideration: ''fractioning'' of the pattern used in the e-beam layout (EBL) the resulting data file size, and the accuracy requirements that have to be met. When the pattern conversion is left to the native EBL software, the performance is not always satisfactory, and alternative approaches must be sought. The reduction of the data volume for circular pattern generation can be achieved by developing software for approximation of circular patterns by rectangular primitives,[14,15] or by assembling a hardware pattern generator for the fast conversion of polar coordinates.[5,16,17]

The zone plate patterns are usually generated in computer-aided design programs that use internal representations for the shapes. While the shapes are stored as high-level fully editable objects, when exported, the file conversion generally place some restriction on the drawing of curves; for example, ICED[18] draws polygons to approximate a circle, and it provides polygons with not more than 64 sides. Several conversions are needed to translate the shapes into a format containing the digital addresses and the instructions for e-beam deflection and blanking. To overcome those design limitations and conversion complexity, we developed a simple program based on C language to generate Cambridge source pattern data (SPD) directly.[19] The basic pattern element types in the Cambridge SPD format, which can be used to approximate circles, are rectangles and polygons.

A simple approximation is that of defining the zones as the union of rectangular areas, and Fig. 1(a) shows a zone plate formed by using rectangles. Rectangles are defined by the coordinates of two diagonal corners. The data file must include coordinate values of all rectangles, and for a zone plate with $N$ zones the number of coordinates is

$$N_{\text{box}} = 2kN_{\text{zones}}^2, \tag{3}$$

where $k$ is the zone-width-to-box-width ratio. The ''staircase'' shaped edge formed by rectangles has a detrimental effect on the zone plate efficiency by removing energy from the coherent central focus. For an ideal phase zone plate, the contribution from the edge of the zone is not very large, thus, the edge roughness caused by the ''staircase'' effect can be made insignificant by increasing the $k$ value. This follows from the equation

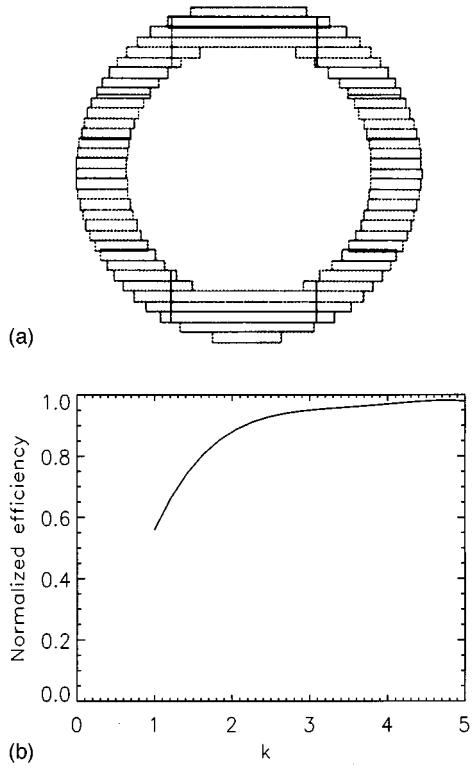


FIG. 1. (a) Example of a zone plate with circular zones approximated by rectangles, here with a zone-width-to-box-width ratio $k = 5$; and (b) the effect of the box $k$ factor on efficiency.

$$\frac{\eta_{\text{box}}}{\eta_{\text{circle}}} = \left(1 - \frac{1}{4k^2}\right)^2, \tag{4}$$

where $\eta_{\text{box}}$ and $\eta_{\text{circle}}$ are the efficiencies of ''box-formed'' and ideal zone plates, respectively [see Fig. 1(b)]. In addition, the roughness of the edges will be smoothed during the lithographic and electroplating processes. However, the approximation of zones with rectangles generates extremely big files. For example, the size of a data file with $k = 3$ and $N = 1860$ is 500 MB, which is difficult to store, convert, and transfer.

A substantial reduction in file size has been achieved by the approximation of circular zones with polygons, and thus, letting the e-beam preprocessor do the job of converting to the line scans. In the Cambridge SPD format, a polygon is defined by a list of the coordinates of all the vertices. The total number of sides of all the polygons in a zone plate is

$$N_{\text{polygon}} = \tfrac{1}{2}mN_{\text{zones}}, \tag{5}$$

where $m$ is the number of sides of a polygon approximating a single zone. For example, for $m = 180$ and $N = 1860$, the Cambridge SPD format data file has only 2 Mb, which is much smaller than that of a box approximation. Generating the zone plate pattern directly in the ASCII code of the SPD format offers a further advantage of bypassing two conversion processes compared with the ICED (or other) programs.

As expected from simple physical optics arguments, the investigation of an image at a point in the principal focal

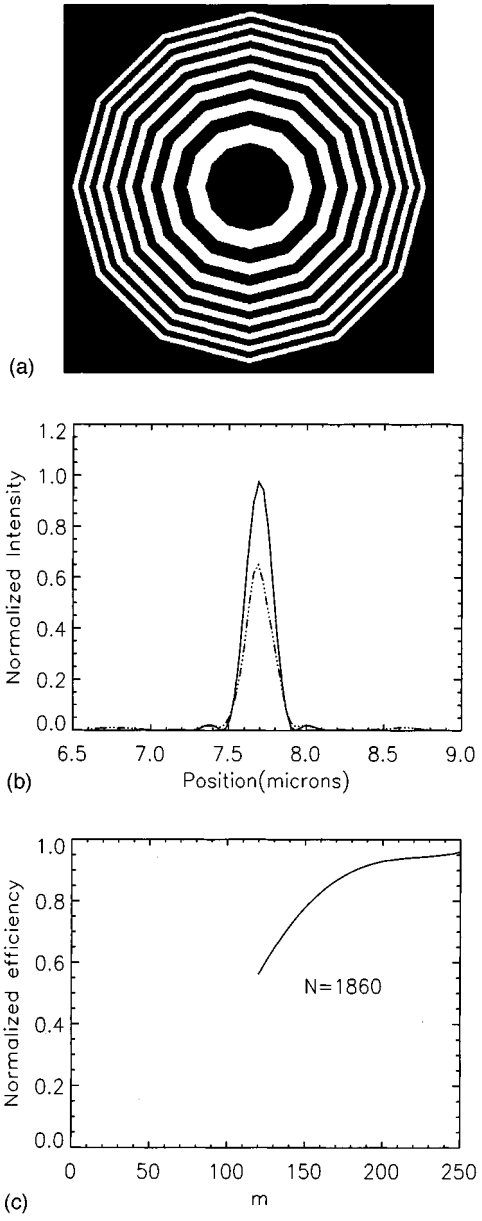


FIG. 2. Examples of a zone plate with circular zones approximated by polygons. (a) Circular zones approximated with polygons of 12 sides; (b) simulated intensity distribution on the focal plane of the FPZP, solid line: circular zones; dashed line: polygon zones ($m=12$); and (c) the effect of the polygon $m$ factor on efficiency for a zone plate with $N=1860$.

plane has shown that the resolution of a polygon-approximated zone plate is not affected by the number of sides, but the efficiency is. The polygons' edges introduce extra scattering structures that diffract intensity away from the focus. Figure 2(a) shows a polygon-shaped ZP and Fig. 2(b) presents simulated intensity distributions in the focal plane for this and an ideal zone plate. The simulation was performed using the XLITH program developed at CXrL.[20] The relative efficiency of a zone plate approximated by polygons of $N$ sides, compared with the efficiency of an ideal zone plate, is given by the equation

$$S=\frac{\eta_{\text{polygon}}}{\eta_{\text{circle}}}=1-\frac{N^2\pi^4}{3m^4}. \tag{6}$$

Using the condition that the Strehl ratio should not be less than 0.8, the acceptable number of polygon sides $m_{\min}$ must satisfy

$$m_{\min}>(5/3)^{1/4}\pi\sqrt{N}\simeq 1.15\pi\sqrt{N}. \tag{7}$$

For example, for a 1860 zone FPZP, $m>154$ ($m=180$ was used in our design). The effect of polygon-shaped zones on the zone plate efficiency is shown in Fig. 2(c).

### B. Zone plate mask fabrication

The master mask was fabricated using the standard mask fabrication process at CXrL. Silicon nitride membranes of $5\times5$ mm$^2$ and 2 $\mu$m thickness were used as the mask pattern carriers. Twenty-one membranes were formed on a 100 mm wafer. The substrates were coated with a layer of chromium (10 nm) and a layer of gold (20 nm) as a plating base. APEX-E resist of 0.4 $\mu$m thickness was used to pattern the mask. Compared to PMMA, APEX-E is a more sensitive positive resist, thus, e-beam writing time is substantially shorter, and the pattern distortions caused by possible drift during long exposures can be reduced. A Leica Cambridge EBMF-10.5 system was used to write the mask in vector scan mode. Several exposures were performed to establish the correct field size, proximity correction, zone width, and dose uniformity within and between the zones. Based on the results of these exposures, a dose range of 6–7 $\mu$C/ cm$^2$ was established, which resulted in ~20 min writing time. A field size of 0.8192 mm was chosen, so nine fields were used to generate zone plates with a diameter of 1860 $\mu$m. Because of the proximity effect, the actual linewidth formed in the resist is larger than programmed, and a linewidth correction had to be applied: an experimentally determined negative bias of 50 nm (linewidth reduction) was introduced for all zones. After exposure and development, the samples were subjected to oxygen reactive ion etching (RIE) to clear the bottom of the patterns. An electroplating process was used to form a 0.3 $\mu$m thick gold absorber. The e-beam fabricated zone plate gold mask patterns are shown in Figs. 3(a) and 3(b).

## III. REPLICATION OF ZONE PLATES USING X-RAY LITHOGRAPHY

### A. Single-layer process

The zone plates were patterned using x-ray proximity printing from the master e-beam mask, and formed by gold electroplating. The zone plate carrier, a silicon nitride membrane formed on a Si wafer, was coated with a Cr/Au plating base and PMMA and exposed through the x-ray mask. The x-ray exposures were performed on the Aladdin synchrotron storage ring at the University of Wisconsin, operating at 800 MeV. The beamline, equipped with a 26 $\mu$m Be window and a 2 $\mu$m SiN filter, provided broadband radiation in the 6–10 Å wavelength region. A mask/wafer gap of 10 $\mu$m was maintained during exposures.

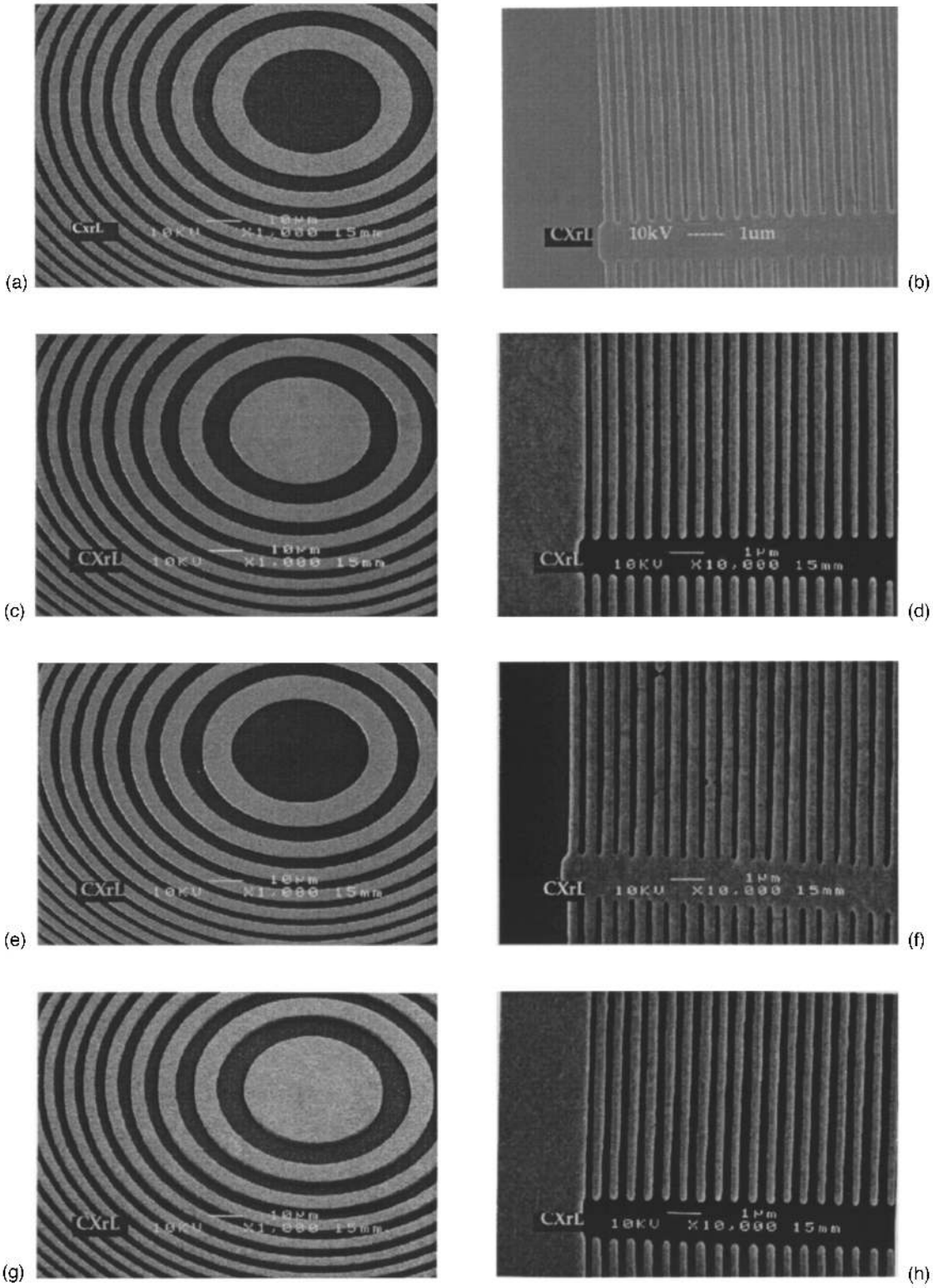


FIG. 3. SEM of the central and outer parts of the FPZP in several replication steps: (a) and (b) e-beam fabrication, $Au_{th}=0.32$ $\mu$m; (c) and (d) first x-ray replication, $Au_{th}=0.55$ $\mu$m; (e) and (f) second x-ray replication, $Au_{th}=0.75$ $\mu$m; and (g) and (h) third x-ray replication, $Au_{th}=1.6$ $\mu$m. After every step, the tone of patterns was reversed and the linewidth was slightly changed due to the process.

The relatively low contrast of the e-beam written x-ray mask (Au thickness 0.3 $\mu$m) was not sufficient to print into 2 $\mu$m thick PMMA directly. Two-step x-ray replication was performed to produce an x-ray mask with sufficient absorber thickness. With every step, the tone of the patterns was reversed and the linewidth was slightly changed due to the RIE procedure. As a result of pattern reversal, a nominal linewidth was obtained after the last replication step. Figure 3

shows the central and the outer regions of the zone plate pattern after sequential replication steps.

FPZPs designed to operate at photon energies of 8 and 20 keV require gold pattern thicknesses of 1.6 and 3.5 $\mu$m, respectively. To fabricate 0.25 $\mu$m and finer zones with such thickness, an appropriate resist annealing process must be employed. Residual resist stress relieved during pattern development can cause collapse of high aspect ratio submicron lines. We used PMMA spin coated to the required thickness and annealed for 1 h at 180 °C in a convection oven, with slow cooling to room temperature. Additionally, the resist adhesion to the substrate is a critical issue in high aspect ratio patterning. PMMA does not have good adhesion to the gold surface used as a plating base, so that a 40 nm thick novolak-based adhesion layer was spun onto the substrate before applying PMMA. After the development of the resist, this layer was removed in oxygen plasma before electroplating. Finally, pattern development is also a very critical step. Development of exposed PMMA was performed in a 1:3 mixture of MIBK and IPA. We used an interrupted development process (8–12 steps) with rinsing after each development step in order to ensure clearing of the bottom of the FPZP pattern everywhere, including fine zones. A low surface tension rinsing solution was used to prevent pattern collapse.[9] Using these techniques, zone plates with 1.6 $\mu$m thick gold zones, 930 $\mu$m radius, and 0.25 $\mu$m outermost zone widths were fabricated. An aspect ratio of 7 in resist has been obtained for the zones with large radius. A higher aspect ratio of 14 can be achieved for zones with smaller radii.[8] The relation between the mechanical stability of the resist pattern and zone radius is a topic of continuing investigation.

### B. Multilevel self-aligned process

For the application of the FPZP in the hard x-ray region (20 keV photons), a pattern with 3.5 $\mu$m thick gold zones is required. We found that a circular pattern with zone radii of 1000 $\mu$m and with 0.25 $\mu$m lines and spaces tends to collapse when PMMA resist thickness exceeded 2 $\mu$m. These limitations are imposed by mechanical properties of this resist and surface tension effects during development. The 2 $\mu$m thick SiN zone plate carrier is transparent to the x rays, and the semiprocessed zone plate can be used as a conformal mask to develop a multilevel self-aligned process.[9]

For the first level, the process described above is performed to fabricate a gold pattern of maximum possible thickness. Negative resist (Shipley XP90104B), exceeding by 1.2 $\mu$m the thickness of the gold pattern, is coated on the top of the structures. A blanket x-ray exposure is performed from the backside (nonpatterned side) of the membrane. The first-layer gold pattern serves here as a contact x-ray mask. During the development of the negative resist, the unexposed areas behind the gold pattern are removed, and the cross-linked exposed resist between the gold lines remains. This resist pattern serves as a mold for the next electroplating step, which increases the total thickness of the FPZP's absorber. Two-layer gold lines with a 0.25 $\mu$m width and a total thickness of 3 $\mu$m have been formed, as shown in Fig. 4.

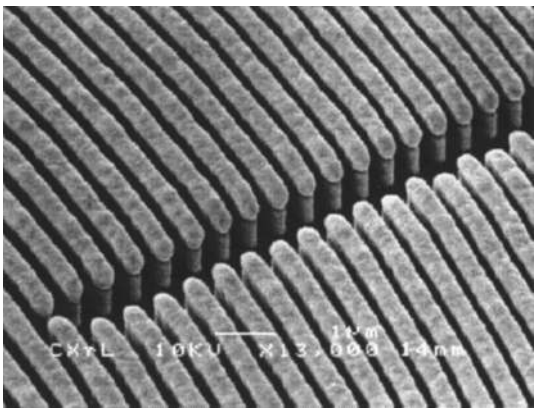


FIG. 4. SEM micrograph of the gold pattern of the FPZP. Two-layer gold was constructed using a self-aligned process to increase the pattern aspect ratio. The total thickness is 3 $\mu$m.

## IV. ZONE PLATE EVALUATION

The performance of a zone plate in terms of resolution and efficiency depends on the accuracy of the actual zones. Since the FZP is essentially a map of the wave front that is synthesized during the imaging process, any inaccuracies in it will translate directly to wave-front errors. The process of fabrication of a zone plate using scanning electron-beam lithography can introduce various aberrations, such as ellipticity, due to slightly different magnification in the $X$ and $Y$ directions, or nonorthogonality of the deflection axes, radial displacement of the zones due to nonlinear beam deflection, or nonconcentricity of the zone rings due to stage or beam drift during writing. These errors are exactly equivalent to the usual third-order aberrations. Pattern displacement can also occur during x-ray replication, due to stress-induced membrane distortions. These defects cause aberrations even for on-axis imaging, and therefore, detract from the resolution and focusing efficiency. The same information is contained in the point spread function for a diffraction-limited source, and the analysis of the image of a point source provides a good test of the quality of the optics. Obviously, the final test of quality is the measurement of the performance as an imaging element in the x rays. However, at-wavelength tests (including star, Foucault knife-edge measurements[21]) obviously require a finished FZP while it is important to be able to assess the quality of the FZP during fabrication.

Moiré patterns of grating structures are widely used as metrological tools. In the case of FZPs, one can use the patterns resulting from two images of the same zone plate superimposed with rotation and/or a shift. This method can be used to determine the geometrical quality of a zone plate,[13] and is essentially equivalent to a shearing interferometry (minus the phase information). Moiré patterns of the actual zone plates can be obtained using the SEM raster structure or by double exposure of a Polaroid film with rotation and translation of the zone plate sample. We used the last technique to evaluate our e-beam fabricated and x-ray replicated

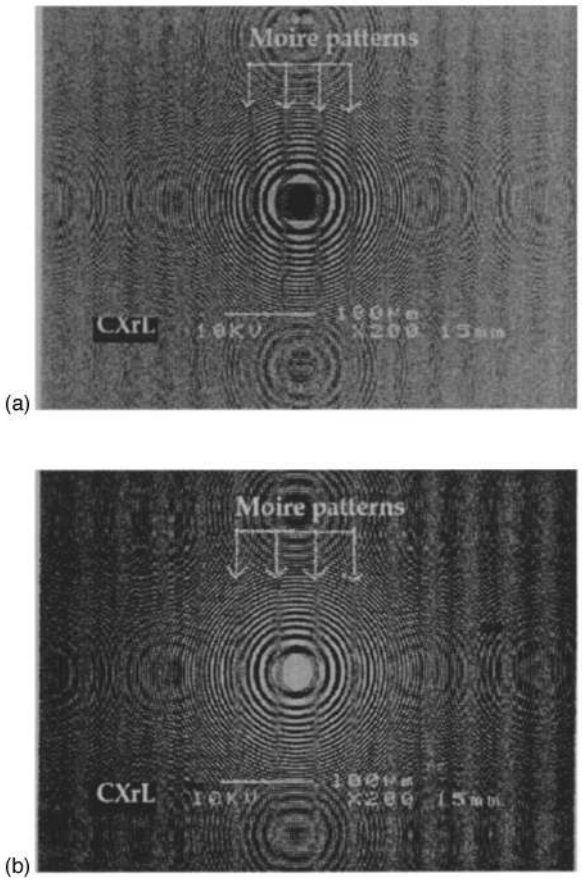


(a)

(b)

FIG. 5. Moiré patterns consisting of a series of vertical parallel straight lines are obtained using double SEM exposure on a Polaroid film with a lateral shift of the sample. (a) The result of an e-beam fabricated FPZP; and (b) the result of an x-ray replicated final FPZP. (The circular moiré pattern is an artifact due to the display raster scan.)

zone plates. Because the scanning electron microscope (SEM) micrographies could not resolve the fine zones at low magnification when the whole zone plate (about 3700 lines) is photographed, moiré patterns of the whole zone plate were not obtained in the large zone number case. Only the quality of center zones (about 200 zones) were evaluated. Figure 5 shows the moiré patterns of the two zone plates, where the series of equidistant parallel straight lines mean that the zone plate is nearly ideal in the photographed part.

## V. SUMMARY

An approach to generate zone plate patterns with large numbers of zones using e-beam writing techniques was demonstrated. It was shown that the approximation of circular zones with polygons is preferable to the box (rectangles) approximation. A relation between the number of sides of an approximating polygon and the number of zones was established to optimize the zone plate efficiency. A program was developed to generate zone plate patterns with large numbers of zones directly in the Cambridge SPD format. A zone plate pattern with 1860 zones was generated using this program and x-ray masks were written on the Leica Cambridge 10.5 e-beam tool installed in CXrL.

Fresnel phase zone plates with 0.25 $\mu$m outermost zone width, 1860 $\mu$m diam, focal length of $f=3$ m (for 8 keV), and 1860 zones were fabricated using a multistep x-ray lithographic replication. The zone material with thicknesses of 1.6 and 3 $\mu$m was formed by gold electroplating to meet phase $\pi$ shift requirements for 8 and 20 keV x rays, respectively. The 1.6 and 3 $\mu$m thick gold lines with the critical dimension of 0.25 $\mu$m were produced utilizing one- and two-level processes, respectively. Moiré metrology has been used for preliminary evaluation of the zone plates.

## ACKNOWLEDGMENTS

This research was supported by Argonne National Laboratory. CXrL is operated under a DARPA contract. The authors are grateful to Mumit Khan, Leonidas Ocola, and Srinivas Bollepalli for fruitful discussions.

[1]E. Spiller, *Soft X-ray Optics* (SPIE Engineering, Bellingham, 1994).
[2]H. Rarback, D. Shu, S. C. Feng, H. Ade, J. Kirz, I. McNulty, D. P. Kern, T. H. P. Chang, Y. Vladimirsky, N. Iskander, D. T. Attwood, K. McQuaid, and Rothman, Rev. Sci. Instrum. **59**, 52 (1988).
[3]G. Schneider, T. Wilhein, B. Nieman, P. Guttmann, T. Schliebe, J. Lehr, H. Aschoff, J. Thieme, D. Rudolph, and G. Schmahl, Proc. SPIE **2516**, 90 (1995).
[4]P. Unger, V. Bogli, and H. Beneking, J. Vac. Sci. Technol. B **6**, 323 (1988).
[5]Y. Vladimirsky, D. Kern, T. H. P. Chang, D. Attwood, H. Ade, J. Kirz, I. McNulty, H. Rarback, and D. Shu, J. Vac. Sci. Technol. B **6**, 311 (1988).
[6]P. Charalambous, P. Anastasi, R. E. Burge, and K. Popova, Proc. SPIE **2516**, 2 (1995).
[7]G. Schneider, T. Schiebe, and H. Archoff, J. Vac. Sci. Technol. B **13**, 3072 (1995).
[8]A. A. Krasnoperova, J. Xiao, F. Cerrina, E. Di Fabrizio, L. Grella, M. Figliomeni, M. Gentili, W. Yun, B. Lai, and E. Gluskin, J. Vac. Sci. Technol. B **11**, 2588 (1993).
[9]A. Krasnoperova, Z. Chen, E. Di Fabrizio, M. Gentili, and F. Cerrina, J. Vac. Sci. Technol. B **13**, 3061 (1995).
[10]E. Di Fabrizio, M. Gentili, L. Grella, M. Baciocchi, A. Krasnoperova, F. Cerrina, W. Yun, B. Lai, and E. Gluskin, J. Vac. Sci. Technol. B **12**, 3979 (1994).
[11]B. Lai, B. Yun, D. Legnini, Y. Xiao, and J. Chrzas, Proc. SPIE **1741**, 180 (1992).
[12]J. Kirz, J. Opt. Soc. Am. **64**, 301 (1974).
[13]Y. Vladimirsky and H. W. P. Koops, J. Vac. Sci. Technol. B **6**, 2142 (1988).
[14]M. Baciocchi, E. Di Fabrizio, M. Gentili, L. Grella, R. Maggiora, L. Mastrogiacomo, and D. Peschiaroli, Jpn. J. Appl. Phys., Part 1 **34**, 6758 (1995).
[15]J. Trotel, J. Vac. Sci. Technol. B **11**, 2397 (1993).
[16]D. P. Kern, P. J. Houzego, P. J. Coane, and T. H. P. Chang, Proc. SPIE **447**, 204 (1984).
[17]E. H. Anderson, V. Boegli, and L. P. Muray, J. Vac. Sci. Technol. B **13**, 2529 (1995).
[18]Graphics Editor For IC Design, IC Editor INC (1990).
[19]EBMF user manual, Leica Cambridge (1993).
[20]J. Z. Guo and F. Cerrina, J. Vac. Sci. Technol. B **9**, 3207 (1991).
[21]F. Berny, Vision Res. **9**, 977 (1969).